AGU PUBLICATIONS

Geophysical Research Letters

RESEARCH LETTER
10.1002/2017GL075029

Key Points:
- The 2005 slab-pull earthquake triggered 9 years of deep-shallow seismicity interactions, while megathrust ruptures initiate a seismic quiescence
- Post slab-pull increased background seismicity is associated with a decrease in GPS eastward velocity, interpreted as interplate decoupling
- Bursts of deep and shallow seismicity are correlated in time, suggesting a lasting physical link between intraslab and interplate ruptures

Supporting Information:
- Supporting Information S1

Correspondence to:
J. Jara,
jorge.jara@univ-grenoble-alpes.fr

Citation:
Jara, J., Socquet, A., Marsan, D., & Bouchon, M. (2017). Long-term interactions between intermediate depth and shallow seismicity in North Chile subduction zone. *Geophysical Research Letters*, *44*. https://doi.org/10.1002/2017GL075029

Received 20 JUL 2017
Accepted 28 AUG 2017
Accepted article online 1 SEP 2017

Long-Term Interactions Between Intermediate Depth and Shallow Seismicity in North Chile Subduction Zone

Jorge Jara[1], Anne Socquet[1], David Marsan[2], and Michel Bouchon[1]

[1]Université Grenoble Alpes, Université Savoie Mont Blanc, CNRS, IRD, IFSTTAR, ISTerre, Grenoble, France, [2]Université Grenoble Alpes, Université Savoie Mont Blanc, CNRS, IRD, IFSTTAR, ISTerre, Chambéry, France

Abstract We document interactions between intermediate depth and interplate seismicity in the North Chile subduction zone, over a 25 year period (1990–2015). We show that the 2005 M_w 7.8 Tarapaca slab-pull earthquake was followed by 9 years of enhanced deep and shallow seismicity, together with the decrease of eastward average GPS velocities and associated interplate coupling, eventually leading to the 2014 M_w 8.1 Iquique megathrust earthquake. In contrast, megathrust ruptures (e.g., M_w 8.0 Antofagasta in 1995, or M_w 8.1 Iquique in 2014) initiate several years of silent background seismicity in the studied area, both at shallow and intermediate depths. The plunge of a rigid slab into a viscous asthenospheric mantle could explain the observed synchronization between deep and shallow seismicity and their long-term interactions.

1. Introduction

Mechanisms leading to large megathrust earthquakes are still not well understood and described. Recent studies showed that a triggering link exists between intermediate depth seismicity and the occurrence of megathrust earthquakes. For example, Lay et al. (2017) showed, from a detailed analysis of source parameters using teleseismic body wave modeling, that the 2016 M_w 7.9 Solomon Islands earthquake was a compound event initiating as a compressional intraslab rupture that coseismically triggered a plate boundary thrust. More intriguing, Bouchon et al. (2016) have observed that precursory seismicity, down to magnitude $M = 1$, at shallow and intermediate depths, occurred synchronously before recent megathrust earthquakes (e.g., M_w 8.8 Maule, Chile, 2010, M_w 9.1 Tohoku-Oki, Japan, 2011, and M_w 8.2 Iquique, Chile, 2014). The reduced magnitude of this precursory seismicity makes direct triggering unlikely, but rather suggests a wider slab deformation or plunge leading to the megathrust rupture. These studies all focus on a preearthquake period that is relatively short in time. Although addressing a time span for deep-shallow seismicity interactions longer than direct coseismic triggering, the latter study remains focused on the 2–3 months preceding the megathrust rupture. However, it has been shown that megathrust earthquakes can be preceded by a long (several months to years) preparation phase (Bouchon et al., 2013; Mavrommatis et al., 2014; Socquet et al., 2017; Yokota & Koketsu, 2015), but interaction between such long precursors and deep processes has not been evidenced so far. Durand et al. (2014) have described seismicity interplay lasting up to 4 years distributed over a wide area in Greece. The authors proposed that an intermediate-depth earthquake started a broad deformation of the slab which led to a large interface earthquake and stretched the overriding plate over far distances. However, until now, no study exists that analyzes the interactions at the decadal scale between deep and shallow subduction earthquakes and their relationship with the megathrust earthquake cycle.

As North Chile subduction undergoes an important seismic activity at intermediate depths (Figure 1) and at the same time is a well-known seismic gap (Béjar-Pizarro et al., 2013; Comte & Pardo, 1991; Métois et al., 2016) with different earthquakes occurring in neighboring parts of the thrust, it represents an excellent case to study this inherent influence and interaction between deep and shallow seismicity. On 13 June 2005, the M_w 7.8 Tarapaca slab-pull earthquake occurred at 100 km depth (Delouis & Legrand, 2007; Peyrat et al., 2006; Peyrat & Favreau, 2010). Nine years later, on 1 April 2014, the M_w 8.1 Iquique megathrust earthquake broke the subduction interface in the same latitude range (Duputel et al., 2015; Hayes et al., 2014; Lay et al., 2014; Ruiz et al., 2014; Schurr et al., 2014; Yagi et al., 2014), following an important foreshock seismic activity (Kato et al., 2016; Meng et al., 2015; Ruiz et al., 2014; Schurr et al., 2014) associated with a slow slip on the subduction

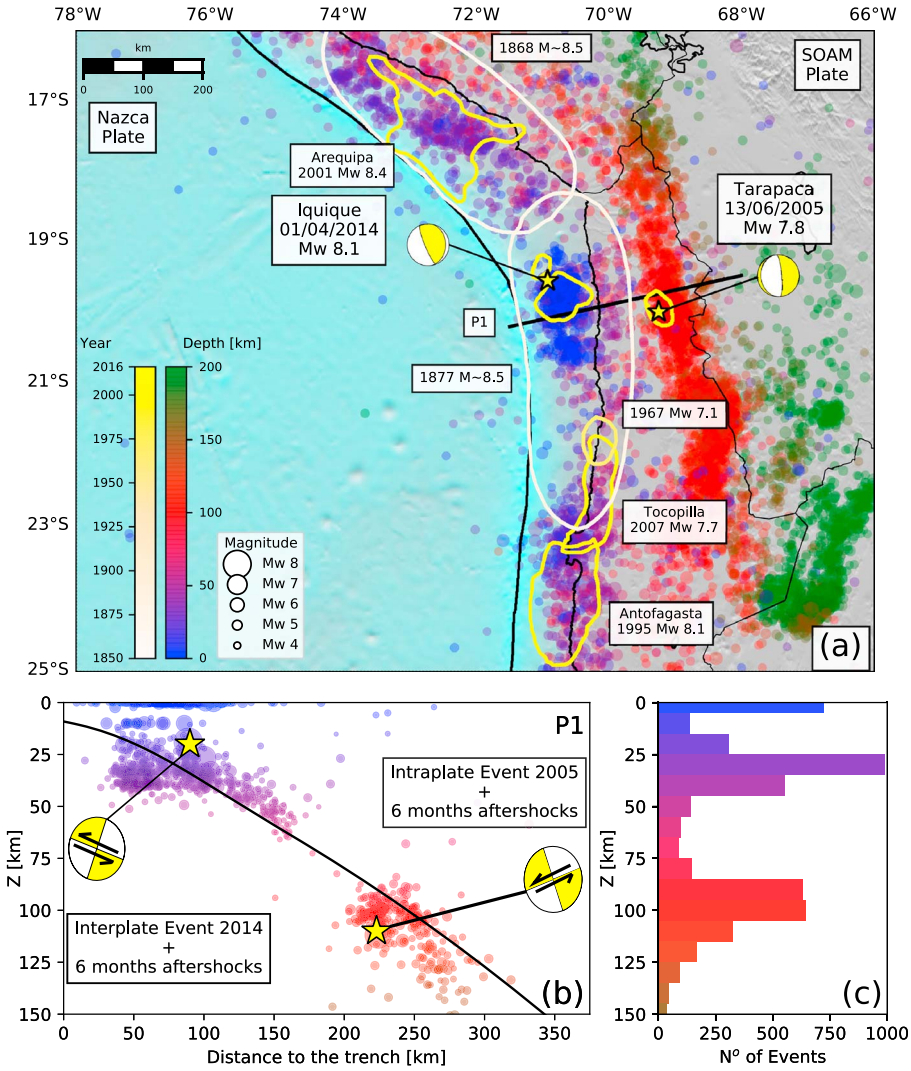

Figure 1. (a) Seismotectonic context of North Chile-South Peru subduction zone. Historical and instrumental rupture areas are color coded as a function of their date of occurrence. Dates and magnitudes of all earthquakes $M > 7.0$ in the area are indicated in squared boxes. Yellow stars and focal mechanisms indicate the epicenters of M_w 7.8 Tarapaca slab-pull earthquake in 2005 (Duputel et al., 2007) and M_w 8.1 Iquique megathrust earthquake in 2014 (Duputel et al., 2015). The 1990–2016 seismicity ($M \geq 4.0$) from the International Seismological Centre (ISC) (2017) is color coded by depth and scaled by magnitude. The black line indicates the location of the profile represented in Figure 1b. (b) Trench-perpendicular profile showing the slab interface from Slab 1.0 (Hayes et al., 2012). Earthquake hypocenters and hemispheric projection of the focal mechanisms are shown in yellow. Also 6 months of aftershocks for each earthquake are plotted, color coded by depth and scaled by magnitude. Tarapaca earthquake fault plane is indicated with a black line above its hypocenter star. (c) Seismicity histogram at depth between 19°S and 21°S, taking into account 10 km to separate each segment.

interface that initiated up to 8 months before the mainshock (Socquet et al., 2017). Here we use both geodetic and seismological data available in the area to characterize the evolution of deformation and seismicity several years before the occurrence of the megathrust and explore the relation between deep and shallow processes, by focusing on the area affected by Tarapaca slab-pull (M_w 7.8, 2005) and Iquique megathrust (M_w 8.1, 2014) earthquakes.

2. Data, Methods, and Results

2.1. GPS Data, Processing, and Average Velocities

GPS data from different networks in South Peru and North Chile (IPOC, LIA "Montessus de Ballore", CAnTO, ISTerre, IGP, and CSN) were processed in double difference using GAMIT 10.5 software (Herring et al., 2015).

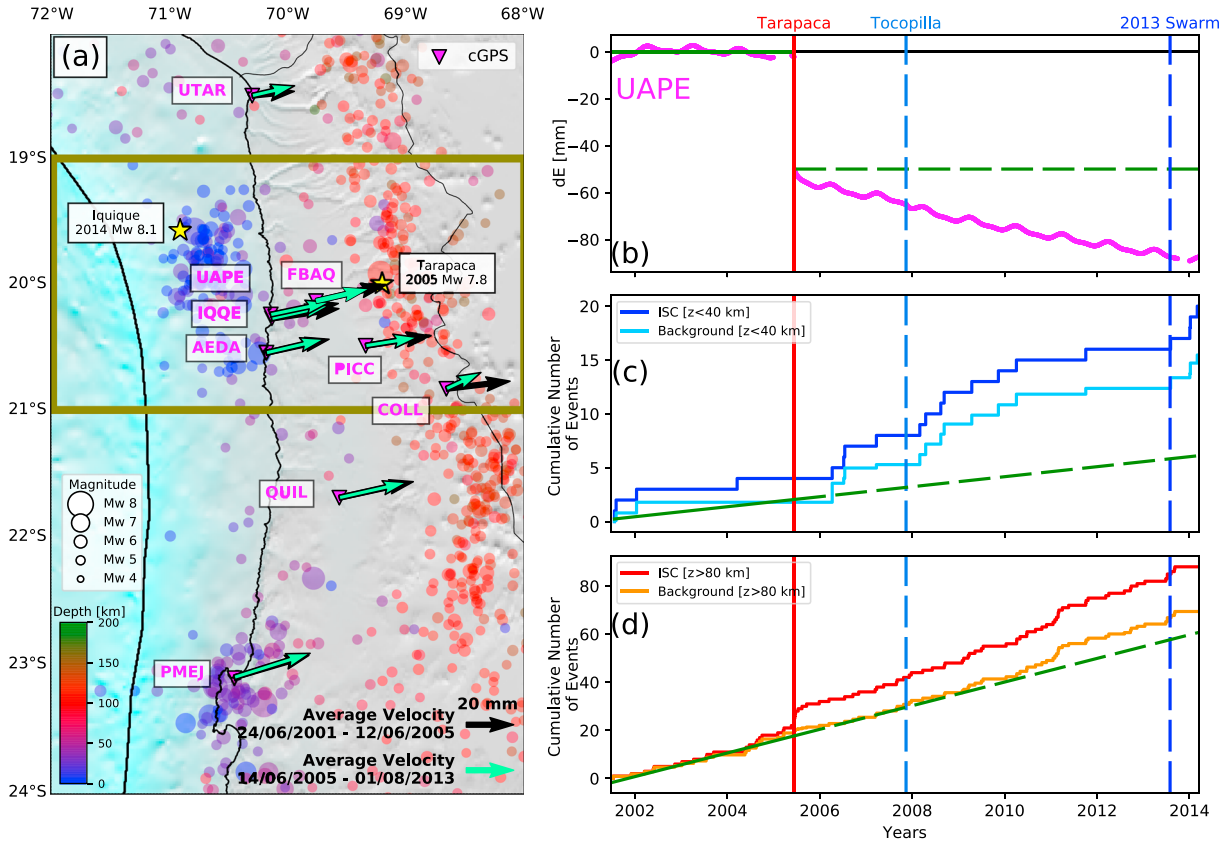

Figure 2. (a) Map of average GPS velocities before (black arrows) and after (green arrows) Tarapaca earthquake 2005. The first period covers 1 day after Arequipa earthquake (2001 M_w 8.4) until 1 day before Tarapaca earthquake. The second period covers 1 day after Tarapaca earthquake up to the swarm activity seen in August 2013, preceding Iquique earthquake. Pink inverted triangles symbolize the location of GPS stations with their respective names at side. The 1990–2016 ISC seismicity is color coded by depth and scaled by magnitude ($M \geq 4.7$, completeness magnitude). The box shows the target zone where the seismicity is studied. Yellow stars indicate the epicenter of Tarapaca and Iquique earthquakes. (b) East component displacement time series of UAPE station, detrended using 2001.44–2005.45 period as reference. Green dashed line shows the coseismically offset projection of the first period trend. Vertical lines point out an earthquake or swarm occurrence: continuous lines represent events that occurred in the study area and dashed events outside it. (c, d) The time evolution of shallow ($z \leq 40$ km) and deep ($z \geq 80$ km) seismicity, respectively. Blue (red) and light blue (orange) are the cumulative number of events for ISC catalog and background seismicity, respectively ($M \geq 4.7$). Green lines show the seismicity trend in the period one (as in Figure 2b and dashed lines show the trend projected to the second period.

The results were mapped into the ITRF 2008 (Altamimi et al., 2011) (see supporting information for details Boehm et al., 2006).

To calculate the average interseismic velocities, the date of the Tarapaca earthquake is taken as the origin date(13 June 2005). The period preceding the earthquake covers from 1 day after the Arequipa earthquake (M_w 8.4, 23 June 2001 Perfettini et al., 2005) until the day before the Tarapaca earthquake. The period following the Tarapaca earthquake starts 1 day after it and ends at the beginning of August 2013, in order to avoid the 8 month precursory phase preceding Iquique earthquake (Socquet et al., 2017). A simple model taking into account the position x_R at a given reference time t_R, the velocity v, and one displacement step for each large earthquake H (Heaviside function), at a given time t_j, is inverted to calculate the velocities, following the Trajectory Model principle (Bevis & Brown, 2014) (equation (1). This model does not consider afterslip or viscoelastic relaxation, due to the fact that there are no clear postseismic signal visible on the GPS time series because of the earthquake depth (100 km) (Figure 2b).

$$x(t) = x_R + v\left(t - t_R\right) + \sum_{j=1}^{n_j} b_j H\left(t - t_j\right) \quad (1)$$

These velocities are calculated for nine stations that have enough data before and after Tarapaca earthquake (Figure 2a, see supporting information for further details on position time series, velocities and errors).

The eastward velocity of UAPE cGPS coastal station decelerates by 4 mm/yr after the occurrence of Tarapaca earthquake (Figure 2b). A similar change in velocity affects most of the cGPS stations within the study area. Coastal stations in this region (IQQE and AEDA) decelerate by 2 to 4 mm/yr, while inland stations (FBAQ, PICC, and COLL) decelarate by ~6 mm/yr (Figure 2a and see supporting information for further details on the velocity values). In comparison, stations located away from the study area (e.g., UTAR and PMEJ) do not exhibit such a change in the average velocity (Figure 2a). We hypothesize that this change in velocity is due to a partial decoupling of the slip interface at depth; we thus aim at searching for futher evidences of this in the seismicity.

2.2. Catalog and Background Seismicity

The ISC event catalog (International Seismological Centre, 2017) from 1990 to 2017 is used to analyze raw and background seismicity. The area analyzed covers the latitude range between 11°S–25°S, and the longitude range 80°W–66°W (Figure 1a). We make use of a method developed by Ogata and Katsura (1993) and Daniel et al. (2008) to compute the catalog completeness magnitude. Because IPOC seismic network was installed in 2007 in Northern Chile, two different periods are considered: from 1990 to 2006 and from 2007 to 2017. Our approach assumes that both periods are characterized by the same b value, thus allowing for a better resolved magnitude of completeness (one for each period). The calculated completeness magnitudes are $M_c = 4.5$ for the first period and $M_c = 4.0$ for the second period (in the whole South Peru-North Chile area considered on which the declustering has been done). We have fixed $M_c = 4.5$ for the whole period 1990–2017 (see supporting information for further details).

An epidemic-type aftershock sequence (ETAS) model is performed to decluster the catalog and estimate the background seismicity (Marsan et al., 2013, 2017). The number of earthquakes (λ) per unit of area (x and y) and unit of time (t) is modeled as the sum of two contributions:

$$\lambda(x, y, t) = \mu(x, y, t) + \nu(x, y, t)\,, \tag{2}$$

where $\nu(x, y, t)$ accounts for triggered earthquakes by a previous one (i.e., aftershocks) and μ is the background seismicity rate (i.e., not triggered by a previous event). The parameters x and y represent the location and t the time of occurrence of each event.

The aftershock rate $\nu(x, y, t)$ is obtained using

$$\nu(x, y, t) = \sum_{i|t_i<t} \nu_i(x, y, t)\,, \tag{3}$$

where t_i is the occurrence time of the ith earthquake; $\nu_i(x, y, t)$ is computed as

$$\nu_i(x, y, t) = \frac{\kappa(m_i)}{(t + c - t_i)^p} \cdot \frac{(\gamma - 1)L(m_i)^{\gamma-1}}{2\pi\left((x - x_i)^2 + (y - y^2) + L(m_i)^2\right)^{(\gamma-1)/2}} \tag{4}$$

That is, the product of the Omori-Utsu law with a power spatial density, with c, γ, and p constants. $L(m) = L_0 \times 10^{0.5(m-4.7)}$ is the characteristic length in kilometer (Elst & Shaw, 2015; Utsu & Seki, 1955) and $\kappa(m)$ is the productivity law, with α constant (Ogata, 1988).

Parameters α, p, c, L_0, and γ are here imposed a priori to realistic values: $\alpha = 2$, $p = 1$, $c = 10^{-3}$ days, $\gamma = 2$, and $L_0 = 1.78$ km. While these parameters can be optimized given the data, in presence or not of a time- and space-varying background rate (Reverso et al., 2015), it is easier and generally sufficient to impose fixed values (see Marsan et al., 2017, for a discussion on this in the context of the northeast Japanese subduction zone). A parameter exploration is performed in the supporting information to evaluate how the results of our analysis depend on this choice. In contrast, parameters κ and $\mu(x, y, t)$ are inverted. The background rate $\mu(x, y, t)$ is calculated as

$$\mu(x, y, t) = \sum_i \frac{\mu\left(x_i, y_i, t_i\right)}{\lambda\left(x_i, y_i, t_i\right)} e^{-\sqrt{(x-x_i)^2+(y-y_i)^2}/\ell} e^{-|t-t_i|/\tau} \times \frac{1}{2\pi\ell^2 a_i} \tag{5}$$

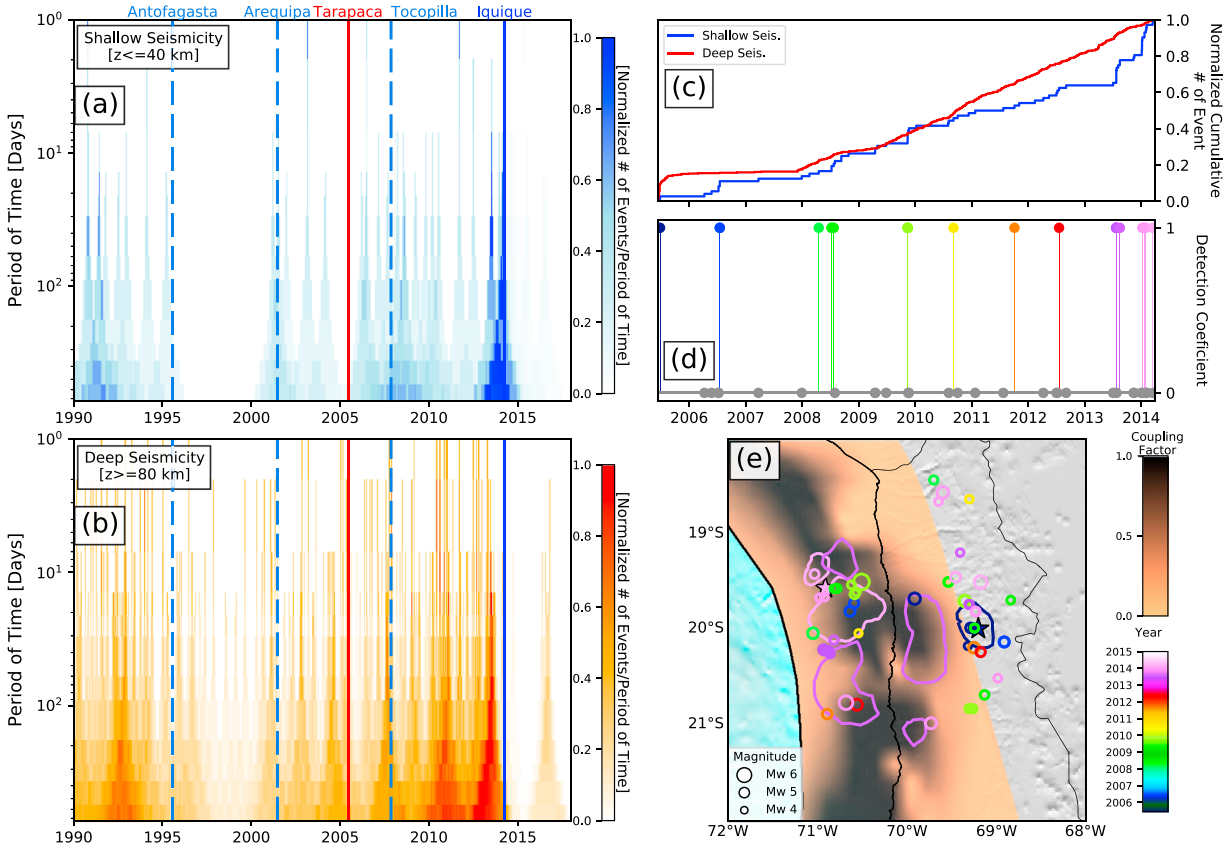

Figure 3. (a, b) The time evolution of normalized background seismicity rate calculated for different periods of reference (from 1 day rate to 2 years rate), for shallow ($z \leq 40$ km) and deep ($z \geq 80$ km) seismicity. Continuous (dashed) lines indicate the time of occurrence of earthquakes into (outside) the study area. Blue (red) are shallow interplate (intermediate depth intraplate) earthquakes. Interactions between shallow and deep seismicity: (c) Normalized cumulative number of events for shallow (blue) and deep (in red) in the study area ($M_c = 4.0$). (d) Synchronization coefficients defined to identify interactions between deep-shallow seismicity. They are color coded by time for 1.0 value (positive interaction) and grey for 0 value (no interaction). (e) Map view of shallow-deep seismicity interaction identified between 14 June 2005 and 1 January 2014, color coded by time. Coupling map is from Métois et al. (2016). Tarapaca and Iquique ruptures (Delouis and Legrand, 2007; Duputel et al., 2015) and 8 month of preseismic slip (Socquet et al., 2017) are plotted and color coded by time.

where ℓ and τ are two smoothing parameters for space and time. The parameter a_i is defined as $a_i = 2\tau - \tau\left(e^{-\frac{t_s - t_i}{\tau}} - e^{-\frac{t_e - t_i}{\tau}}\right)$. Parameters t_s and t_e represent the starting and ending time of the catalog. Parameter κ is computed as

$$\kappa = \frac{\sum_i 1 - \frac{\mu(x_i, y_i, t_i)}{\lambda(x_i, y_i, t_i)}}{\sum_i e^{\alpha m_i}\left(\ln\left(t_e + c - t_i\right) - \ln c\right)} \tag{6}$$

We have used a smoothing length ℓ of 100 km and smoothing duration τ of 100 days to preserve the potential accelerations in the catalog (Marsan et al., 2017).

We perform the declustering for the whole area (Figure 1a) and eventually focus on the region affected by the two mainshocks (box in Figure 2a) This smaller area is characterized by a slightly larger M_c of 4.7 compared to the whole area on which the declustering has been performed (see supporting information S1 for further details). Thus, the seismicity with magnitude over 4.7 is selected from the regional declustered catalog to perform the analysis on the specific zone.

We separated shallow ($z \leq 40$ km) and deep ($z \geq 80$ km) background seismicity (Figures 2c and 2d).This depth selection has been made to better separate deep and shallow events by avoiding the seismicity between 40 and 80 km at depth, that is, a depth range with very little seismicity (Figure 1c). It is obvious from Figure 2d that the declustering mostly removes the aftershocks following the Tarapaca earthquake. Despite this, a clear increase both in deep and shallow background seismicity can be seen after the 2005 Tarapaca earthquake (shallow seismicity in 2006 and deep seismicity in 2011). In order to characterize its temporal variability, seismicity rates are calculated for reference periods ranging from 1 day to 2 years. Figures 3a and 3b offer

a view of deep and shallow seismicity rates computed for different time windows, ranging from 1 day to 2 years, over 25 year time span. It shows that the 9 year period of increased deep and shallow seismicity following 2005 Tarapaca slab-pull earthquake, is followed by a period of quiescence after the occurrence of the 2014 earthquake. Similarly, the 1995 Antofagasta earthquake marks the limit between an important seismic activity before, and no background seismicity after. It also allows one to observe that the seismicity release does not occur steadily in the long-term, but rather through a series of pulses.

3. Discussion

3.1. A Change in Deformation and Seismicity After Tarapaca Slab-Pull Earthquake

After the 2005 Tarapaca earthquake, a significant change in the surface deformation can be observed (Figure 2a). The reduction in eastward velocity could be related to post-seismic deformation following the slab-pull event (e.g., poroelastic rebound e.g., Jonsson et al., 2003; Peltzer et al., 1998, afterslip e.g., Hsu et al., 2006, or mantle's viscoelastic relaxation e.g., Khazaradze et al., 2002; Klein et al., 2016). Given the fact that the earthquake occurred at 100 km depth, it is likely that poroelastic rebound, which usually takes place at shallow depths within structural complexities of the fault (Jonsson et al., 2003; Peltzer et al., 1998), does not exist or is hardly detectable in the surface deformation field (if any occurs). Part of this velocity reduction of the stations is located far from the coast (more than 6 mm/yr after the earthquake). Given the fact that the change in velocity affects a large area, a viscoelastic relaxation has been invoked (Bie et al., 2017), although it is not possible to observe the associated long-term typical exponential-like transient in the GPS time series, that is usually associated with this type of mechanism. Whatever the mechanism, such long-term changes in the surface displacement rates suggest that Tarapaca intraplate earthquake had an important impact on the surface deformation field and therefore on the amount and pattern of the interseismic compression in the upper plate and at the plate boundary. This broad change in surface deformation generates a velocity reduction of ∼4 mm/yr at coastal stations and likely modifies the stress regime close to the plate boundary, enhancing unclamping as well as a change in the coupling on the subduction interface. Until recently, no slow slip events had been reported in the area. Ruiz et al. (2014) and Schurr et al. (2014) have shown a strong transient deformation, for which the aseismic nature is debated, during the weeks preceding the occurrence of Iquique earthquake, and Socquet et al. (2017) showed that an 8 month aseismic slow slip preceded the earthquake. These slow slip events have also been observed by the analysis of repetitive earthquakes. Kato et al. (2016), Meng et al. (2015), and Yagi et al. (2014) have pointed out the occurrence of aseismic deformation over the same period as Ruiz et al. (2014). Taking a longer period of time, Kato et al. (2016) have detected an aseismic slip starting in 2008 with a continuous rate of 0.67 mm/yr until the 2013 seismic swarm. Because the average velocity field is calculated up to the 2013 swarm (avoiding the precursory phase of Iquique earthquake, Socquet et al., 2017), the observed reduction of coastal velocities is compatible with Kato et al. (2016) and we interpret this behavior as a reduction of coupling on the subduction interface.

Associated with the decrease in eastward GPS velocities, an increase in seismicity rate is observable both at deep and shallow depths during the interearthquake period, either in the whole ISC catalog or in the background seismicity (Figures 2 and 3). The background seismicity is usually considered to be a proxy of the tectonic loading in a specific area, so that any important deviation from the average trend can be associated with slow slip events and fluid or magmatic migrations (Marsan et al., 2017). This therefore suggests an increase in the tectonic loading, which is compatible with the observed decrease in GPS eastward velocity interpreted as an interplate decoupling (and therefore an increased creep on the subduction interface). Interestingly, this increase in background seismicity rates concerns both shallow and deep earthquakes, suggesting that a link exists between shallow and deep seismic responses.

3.2. Long-Term Interactions Between Shallow and Intraslab Seismicity

Figures 3a and 3b offer a view of the background seismicity rates over a 25 year time span, for deep and shallow seismicity. Before Antofagasta megathrust earthquake (M_w 8.0, 1995 Delouis et al., 1997), both deep and shallow background activities are significant. After this earthquake, the study area entered in a silent period until the occurrence of the Arequipa earthquake in mid-2001 in South Peru (M_w 8.4 Perfettini et al., 2005). The Arequipa earthquake initiates the reactivation of a subtle background seismic activity that accelerates at depth in the months preceding Tarapaca slab-pull earthquake. The Tarapaca intraslab earthquake triggers an increase in both deep and shallow seismicity rates. At the end of 2007, in the southern part of the gap, the Tocopilla earthquake (M_w 7.7 Béjar-Pizarro et al., 2010; Peyrat et al., 2010) triggers a burst of shallow seismicity. Then, 4 years before Iquique megathrust earthquake, the deep seismicity rate increases, followed in August

2013 by the increase of the shallow background seismicity rate, 8 months before the mainshock. In April 2014, Iquique megathrust earthquake ruptures a large part of the plate interface and concludes a period of enhanced deep and shallow background seismic activity that initiated 9 years before with the occurrence of Tarapaca slab-pull earthquake. Since the occurrence of the Iquique megathrust in April 2014 (up to now), the background seismic activity is almost zero, at least at $M_c = 4.7$.

Global tectonic models propose different forces leading the Earth's convection. One primary force responsible for this process is that generated by the slab subducting beneath the lithosphere. These models have shown that a relationship exists between the "slab-pull" force and the processes occurring in the seismogenic zone (e.g., Bilek et al., 2005; Conrad et al., 2004; Conrad & Lithgow-Bertelloni, 2002; Spence, 1987). From a local seismotectonic point of view, models describe interactions between interplate and intraplate events. These models depend on how far in the seismic cycle the thrust is. Prior to a thrust event, the stress regime at intermediate depth exhibits tensional behavior generating preferentially slab-pull earthquakes. Conversely, after a thrust earthquake, the stress regime changes to the opposite, generating compressional slab-push events (e.g., Astiz & Kanamori, 1986; Astiz et al., 1988; Dmowska et al., 1988; Lay et al., 1989; Lemoine et al., 2001; Malgrange & Madariaga, 1983). The observed period of enhanced deep and shallow seismicity after an intraslab event and silent periods following megathrust earthquakes might be explained by such mechanical models. Usually, previous works focus the attention in earthquake occurrence. Slab-push earthquakes in subduction zones have been documented after shallower activity (Fuenzalida et al., 2013; Lemoine et al., 2001, 2002; Peyrat et al., 2010; Ruiz & Madariaga, 2011). However, the quiescent periods have been less reported. Here we suggest that the observed arrest of slab-pull seismicity ($M_c = 4.7$) could be explained by a similar mechanism. The observed increase in the seismicity (at deep and shallow depths) after the slab-pull rupture, would be controlled by a mechanism of afterslip and decoupling on the subduction interface, while the silent period following megathrust ruptures, by clamping of the faults cutting the slab through an increase of compressive stress along the slab. In the shallow part, a possible mechanism could be the lack of interplate earthquakes in the area that previously ruptured coseismically because of the large amount of stress released during the earthquake, as it has been observed after Tohoku-anOki earthquake (Asano et al., 2011).

3.3. Synchronization of Deep and Shallow Seismicity

Another interesting feature revealed by Figures 3a and 3b is the fact that the background seismic activity is not continuous in time, but rather occurs by bursts, both for shallow and deep events. These swarms are usually associated with aseismic episodes (Reverso et al., 2015, 2016). The shallow bursts are associated with swarms detected in 2006, 2008, and 2013 (see supporting information S1 for details), which may indicate the occurrences of SSEs, plus a few isolated background earthquakes between 2005 and 2014 that occur as a response to tectonic loading (Figure 3). The fact that both deep and shallow bursts occur within a short time span suggests some type of interaction between deep and shallow seismic activities. In order to further explore these potential interactions, we have tried to characterize the correlation of shallow seismicity with deep seismicity. Using the cumulative number of earthquakes for shallow ($z \leq 40$ km) and deep ($z \geq 80$ km) seismicity (Figure 3c), we look for each shallow earthquake if a deep earthquake occurred in the 2 days preceding it (see supporting information S1 for details in terms of time window selection, completeness magnitude, and probability of synchronizations by chance). If so, a value 1 is assigned, otherwise this value is 0 (Figure 3d). In this part of the work, all the seismicity over magnitude 4.0 is considered. Doing so, 16 interactions have been detected (Figure 3d), which is 133% of the number of interactions expected to occur by pure chance (see Supporting Information S1 for further details on the statistical significance of the observed synchronizations). The results shown by Bouchon et al. (2016) (four synchronizations) are replicated from January to 1 April 2014. Before that 12 additional deep and shallow seismicity synchronizations are detected. The identified interactions correspond either to swarms (e.g., 2006, 2008, and 2013) or background earthquakes (e.g., 2009 and 2011). Three areas in the shallow part of the megathrust are systematically activated, surrounding the area that ruptured during the 2014 Iquique earthquake. We have in total 16 synchronization episodes where we can observe 24 shallow earthquakes. About 84% occurred in areas with a coupling factor between 0.3 and 0.8 (Métois et al., 2016), i.e., areas not fully coupled (Figure 3, see supporting information S1 for details in coupling model).

The 16 episodes of deep-shallow seismicity synchronization (Figures 3d and 3e) may represent, as proposed by Bouchon et al. (2016), a slab deformation and plunge preceding the shallow burst activity. These interactions help to identify where the aseismic deformation is occurring. Interestingly, the shallow seismicity triggered by these interactions is located in areas that are at the transition between high and low interseismic coupling (Figure 3e). Moreover, these triggered seismic events are all located at the border of the areas that have been

shown to aseismically slip during the 8 months preceding the 2014 Iquique megathrust, or within the area that slipped coseismically (purple and pink contours, respectively, in Figure 3e (Socquet et al., 2017)). This precursory activity marks the area that started to slip in the 9 years preceding the Iquique interface earthquake, as a response to Tarapaca slab-pull earthquake.

The observed synchronization of seismic activity at intermediate depth and on the shallow subduction interface questions our understanding of the interaction mechanisms between deep and shallow processes. The fact that Iquique earthquake megathrust occurred 9 years after the Tarapaca slab-pull earthquake, rather pleads for a slow deformation process taking place within the slab, possibly with a transient acceleration phases, marked by these synchronized pulses of deep and shallow seismicity, rather than a simple static triggering (e.g., Coulomb stress increase) that is difficult to invoke at such spatial and temporal distances. Our observations suggest that there exists a strong link between interplate and intraslab seismicity. The presence of a rigid slab decoupled from the surrounding asthenospheric mantle would favor the stress migration and aseismic deformation propagation from the slab to the subduction interface. Such decoupling would be allowed by a low-viscosity channel, permitting transient deep rapid sliding of the slab, as it has been proposed down to 70 km depth by Klein et al. (2016) to explain the postseismic GPS time series following Maule earthquake M_w 8.8 in Chile.

4. Conclusions

This study presents clear evidence that strong interactions exist between the occurrence of intermediate depth and shallow seismicity in subduction zones. The occurrence of the Tarapaca slab-pull earthquake initiated a 9 year period of deep-shallow seismicity interactions in a burst form, associated with a decrease of the interplate interseismic coupling, eventually leading to the 2014 M_w 8.1 Iquique megathrust earthquake. Moreover, megathrust ruptures (Antofagasta 1995 and Iquique 2014) initiate long periods (several years) of silent background seismicity, both on the plate interface, probably due to decoupling associated with postseismic afterslip (Chlieh et al., 2007; Pritchard & Simons, 2006), and at intermediate depth, probably by clamping of the faults cutting the slab through an increase of compressive stress (e.g., Astiz et al., 1988; Astiz & Kanamori, 1986; Dmowska et al., 1988; Lay et al., 1989). After a few years of silence, the background seismicity resumes both at intermediate and shallow depths, and initiates a new cycle of deep shallow interactions.

If the seismogenic zone is already highly loaded, the occurrence of a large intermediate-depth intraslab earthquake could trigger or clock-advance a megathrust event by enhancing the occurrence of foreshocks and preslip on the subduction interface as a response to stress migration. Conversely, if the interplate contact is not ready to nucleate a megathrust earthquake, our results suggest that the slab deformation and plunge accommodated by the occurrence of a large intraslab event generate an increased activity of deep and shallow seismicity that are most often synchronized. It changes the stress conditions in the slab, up to the shallower depths. As a result, a decrease of interseismic coupling (i.e., acceleration of slow slip on the plate interface) may change the average GPS velocities and increase the background seismicity rate, both processes taking place as a series of bursts. Such a long-term interaction between slab-pull and shallow earthquakes helps understand the mechanisms leading to a megathrust earthquake. If this were true, the occurrence of intermediate-depth earthquakes could therefore significantly increase the probability of a possible future rupture in megathrust.

Acknowledgments
The authors thank the International Plate Boundary Observatory Chile (IPOC,www.ipoc-network.org), Laboratoire International Associé "Montessus de Ballore" (www.liamb.net), Central Andean Tectonic Observatory Geodetic Array (CAnTO, http://www.tectonics.caltech.edu/resources/continuous_gps.html), and Instituto Geofísico del Perú (www.igp.gob.pe) for making the raw GPS data available. Also, authors thank the Centro Sismológico Nacional de Chile (CSN, www.csn.uchile.cl) that provide the Chilean seismicity catalog analyzed during this study. Jorge Jara acknowledges a PhD scholarship granted by Chilean National Science Cooperation (CONICYT) through "Becas Chile" Program. The authors thank J.M. Nocquet for making PYACS software available, as well as Bogdan Enescu and an anonymous reviewer for their constructive comments on the manuscript.

References

Altamimi, Z., Collilieux, X., & Métivier, L. (2011). ITRF2008: An improved solution of the international terrestrial reference frame. *Journal of Geodesy*, *85*(8), 457–473. https://doi.org/10.1007/s00190-011-0444-4

Asano, Y., Saito, T., Ito, Y., Shiomi, K., Hirose, H., Matsumoto, T., ... Sekiguchi, S. (2011). Spatial distribution and focal mechanisms of aftershocks of the 2011 off the Pacific Coast of Tohoku earthquake. *Earth, Planets and Space*, *63*(7), 29. https://doi.org/10.5047/eps.2011.06.016

Astiz, L., & Kanamori, H. (1986). Interplate coupling and temporal variation of mechanisms of intermediate-depth earthquakes in Chile. *Bulletin of the Seismological Society of America*, *76*(6), 1614–1622.

Astiz, L., Lay, T., & Kanamori, H. (1988). Large intermediate-depth earthquakes and the subduction process. *Physics of the Earth and Planetary interiors*, *53*(1), 80–166. https://doi.org/10.1016/0031-9201(88)90138-0

Béjar-Pizarro, M., Carrizo, D., Socquet, A., Armijo, R., Barrientos, S., Bondoux, F., ... Vigny, C. (2010). Asperities and barriers on the seismogenic zone in North Chile: State-of-the-art after the 2007 M_w 7.7 Tocopilla earthquake inferred by GPS and InSAR data. *Geophysical Journal International*, *183*(1), 390–406. https://doi.org/10.1111/j.1365-246x.2010.04748.x

Béjar-Pizarro, M., Socquet, A., Armijo, R., Carrizo, D., Genrich, J., & Simons, M. (2013). Andean structural control on interseismic coupling in the North Chile subduction zone. *Nature Geoscience*, *6*(6), 462–467. https://doi.org/10.1038/ngeo1802

Bevis, M., & Brown, A. (2014). Trajectory models and reference frames for crustal motion geodesy. *Journal of Geodesy*, *88*(3), 283–311. https://doi.org/10.1007/s00190-013-0685-5

Bie, L., Ryder, I., & Metois, M. (2017). Deep postseismic viscoelastic relaxation excited by an intraslab normal fault earthquake in the Chile subduction zone. *Tectonophysics*, *712–713*, 729–735. https://doi.org/10.1016/j.tecto. 2017.07.012

Bilek, S. L., Conrad, C. P., & Lithgow-Bertelloni, C. (2005). Slab pull, slab weakening, and their relation to deep intra-slab seismicity. *Geophysical Research Letters*, *32*, L1430. https://doi.org/10.1029/2005GL022922

Boehm, J., Werl, B., & Schuh, H. (2006). Troposphere mapping functions for GPS and very long baseline interferometry from European Centre For Medium-range Weather Forecasts operational analysis data. *Journal of Geophysical Research*, *111*, B0240. https://doi.org/10.1029/2005JB003629

Bouchon, M., Durand, V., Marsan, D., Karabulut, H., & Schmittbuhl, J. (2013). The long precursory phase of most large interplate earthquakes. *Nature Geoscience*, *6*(4), 299–302. https://doi.org/10.1038/ngeo1770

Bouchon, M., Marsan, D., Durand, V., Campillo, M., Perfettini, H., Madariaga, R., & Gardonio, B. (2016). Potential slab deformation and plunge prior to the Tohoku, Iquique and Maule earthquakes. *Nature Geoscience*, *9*(5), 380–383. https://doi.org/10.1038/ngeo2701

Chlieh, M., Avouac, J.-P., Hjorleifsdottir, V., Song, T.-R. A., Ji, C., Sieh, K., ... Galetzka, J. (2007). Coseismic slip and afterslip of the great M_w 9.15 Sumatra–Andaman earthquake of 2004. *Bulletin of the Seismological Society of America*, *97*(1A), S152—S173. https://doi.org/10.1785/0120050631

Comte, D., & Pardo, M. (1991). Reappraisal of great historical earthquakes in the Northern Chile and Southern Peru seismic gaps. *Natural hazards*, *4*(1), 23–44. https://doi.org/10.1007/BF00126557

Conrad, C. P., & Lithgow-Bertelloni, C. (2002). How mantle slabs drive plate tectonics. *Science*, *298*(5591), 207–209. https://doi.org/10.1126/science.1074161

Conrad, C. P., Bilek, S., & Lithgow-Bertelloni, C. (2004). Great earthquakes and slab pull: Interaction between seismic coupling and plate–slab coupling. *Earth and Planetary Science Letters*, *218*(1), 109–122. https://doi.org/10.1016/ S0012-821X(03)00643-5

Daniel, G., Marsan, D., & Bouchon, M. (2008). Earthquake triggering in Southern Iceland following the June 2000 M_s 6.6 doublet. *Journal of Geophysical Research: Solid Earth*, *113*, B05310. https://doi.org/10.1029/2007JB005107

Delouis, B., & Legrand, D. (2007). M_w 7.8 Tarapaca intermediate depth earthquake of 13 June 2005 (Northern Chile): Fault plane identification and slip distribution by waveform inversion. *Geophysical Research Letters*, *34*, L01304. https://doi.org/10.1029/2006GL028193

Delouis, B., Monfret, T., Dorbath, L., Pardo, M., Rivera, L., Comte, D., ... Cisternas, A. (1997). The $M_w = 8.0$ Antofagasta (Northern Chile) earthquake of 30 July 1995: A precursor to the end of the large 1877 gap. *Bulletin of the Seismological Society of America*. *87*(2), 427–445.

Dmowska, R., Rice, J. R., Lovison, L. C., & Josell, D. (1988). Stress transfer and seismic phenomena in coupled subduction zones during the earthquake cycle, *Journal of Geophysical Research*. *93*, 7869–7884. https://doi.org/10.1029/JB093iB07p07869

Duputel, Z., Jiang, J., Jolivet, R., Simons, M., Rivera, L., Ampuero, J.-P., ... Minson, S. E. (2015). The Iquique earthquake sequence of April 2014: Bayesian modeling accounting for prediction uncertainty. *Geophysical Research Letters*, *42*, 7949–7957. https://doi.org/10.1002/2015GL065402

Durand, V., Bouchon, M., Floyd, M. A., Theodulidis, N., Marsan, D., Karabulut, H., & Schmittbuhl, J. (2014). Observation of the spread of slow deformation in Greece following the breakup of the slab. *Geophysical Research Letters*, *41*, 7129–7134. https://doi.org/10.1002/2014GL061408

Elst, N. J., & Shaw, B. E. (2015). Larger aftershocks happen farther away: Nonseparability of magnitude and spatial distributions of aftershocks, *Geophysical Research Letters*, *42*, 5771–5778. https://doi.org/10.1002/2015GL064734

Fuenzalida, A., Schurr, B., Lancieri, M., Sobiesiak, M., & Madariaga, R. (2013). High-resolution relocation and mechanism of aftershocks of the 2007 Tocopilla (Chile) earthquake. *Geophysical Journal International*, *194*, 1216–1228. https://doi.org/10.1093/gji/ggt163

Hayes, G. P., Wald, D. J., & Johnson, R. L. (2012). Slab 1.0: A three-dimensional model of global subduction zone geometries. *Journal of Geophysical Research*, *117*, B01302. https://doi.org/10.1029/2011JB008524

Hayes, G. P., Herman, M. W., Barnhart, W. D., Furlong, K. P., Riquelme, S., Benz, H. M., ... Samsonov, S. (2014). Continuing megathrust earthquake potential in Chile after the 2014 Iquique earthquake. *Nature*, *512*(7514), 295–298. https://doi.org/10.1038/nature13677

Herring, T., King, R. W., Floyd, M. A., & McClusky, S. C. (2015). *GAMIT, Reference Manual*, MA: Departament of Earth, Atmospheric, and Planetary Sciences, Massachusetts Institute of Technology.

Hsu, Y.-J., Simons, M., Avouac, J.-P., Galetzka, J., Sieh, K., Chlieh, M., ... Bock, Y. (2006), Frictional afterslip following the 2005 Nias-Simeulue earthquake, Sumatra, *Science*, *312*(5782), 1921–1926. https://doi.org/10.1126/science.1126960

International Seismological Centre (2017). *On-line Bulletin*, Thatcham, UK: International Seismological Centre. http://www.isc.ac.uk.

Jonsson, S., Segall, P., Pedersen, R., & Björnsson, G. (2003). Post-earthquake ground movements correlated to pore-pressure transients. *Nature*, *424*(6945), 179–183. https://doi.org/10.1038/nature01776

Kato, A., Fukuda, J., Kumazawa, T., & Nakagawa, S. (2016). Accelerated nucleation of the 2014 Iquique, Chile M_w 8.2 earthquake. *Scientific reports*, *6*, 24792. https://doi.org/10.1038/srep24792

Khazaradze, G., Wang, K., Klotz, J., Hu, Y., & He, J. (2002). Prolonged post-seismic deformation of the 1960 Great Chile earthquake and implications for mantle rheology. *Geophysical Research Letters*, *29*(22), 2050. https://doi.org/10.1029/2002GL015986

Klein, E., Fleitout, L., Vigny, C., & Garaud, J. (2016). Afterslip and viscoelastic relaxation model inferred from the large-scale post-seismic deformation following the 2010 M_w 8.8 Maule earthquake (Chile). *Geophysical Journal International*, *205*, 1455–1472. https://doi.org/10.1093/gji/ggw086

Lay, T., Astiz, L., Kanamori, H., & Christensen, D. H. (1989). Temporal variation of large intraplate earthquakes in coupled subduction zones. *Physics of the Earth and Planetary Interiors*, *54*(3-4), 258–312. https://doi.org/10.1016/0031-9201(89)90247-1

Lay, T., Yue, H., Brodsky, E. E., & An, C. (2014). The 1 April 2014 Iquique, Chile, M_w 8.1 earthquake rupture sequence. *Geophysical Research Letters*, *41*, 3818–3825. https://doi.org/10.1002/2014GL060238

Lay, T., Ye, L., Ammon, C. J., & Kanamori, H. (2017). Intraslab rupture triggering megathrust rupture coseismically in the 17 December 2016 Solomon Islands M_w 7.9 earthquake. *Geophysical Research Letters*, *44*, 1286–1292. https://doi.org/10.1002/2017GL072539

Lemoine, A., Madariaga, R., & Campos, J. (2001). Evidence for earthquake interaction in Central Chile: the July 1997–September 1998 sequence. *Geophysical Research Letters*, *28*(14), 2743–2746. https://doi.org/10.1029/2000GL012314

Lemoine, A., Madariaga, R., & Campos, J. (2002). Slab-pull and slab-push earthquakes in the Mexican, Chilean and Peruvian subduction zones. *Physics of the Earth and Planetary Interiors*, *132*(1), 157–175. https://doi.org/10.1016/s0031-9201(02)00050-x

Malgrange, M., & Madariaga, R. (1983). Complex distribution of large thrust and normal fault earthquakes in the Chilean subduction zone. *Geophysical Journal International*, *73*(2), 489–505. https://doi.org/10.1111/j.1365-246x.1983.tb03326.x

Marsan, D., Bouchon, M., Gardonio, B., Perfettini, H., Socquet, A., & Enescu, B. (2017). Change in seismicity along the Japan trench, 1990–2011, and its relationship with seismic coupling. *Journal of Geophysical Research: Solid Earth*, *122*, 4645–4659. https://doi.org/10.1002/2016JB013715

Marsan, D., Reverso, T., Helmstetter, A., & Enescu, B. (2013). Slow slip and aseismic deformation episodes associated with the subducting Pacific Plate offshore Japan, revealed by changes in seismicity. *Journal of Geophysical Research: Solid Earth*, *118*, 4900–4909. https://doi.org/10.1002/jgrb.50323

Mavrommatis, A. P., Segall, P., & Johnson, K. M. (2014). A decadal-scale deformation transient prior to the 2011 M_w 9.0 Tohoku-oki earthquake. *Geophysical Research Letters*, *41*, 4486–4494. https://doi.org/10.1002/2014GL060139

Meng, L., Huang, H., Bürgmann, R., Ampuero, J. P., & Strader, A. (2015). Dual megathrust slip behaviors of the 2014 Iquique earthquake sequence. *Earth and Planetary Science Letters*, *411*, 177–187. https://doi.org/10.1016/j.epsl.2014.11.041

Métois, M., Vigny, C., & Socquet, A. (2016). Interseismic coupling, megathrust earthquakes and seismic swarms along the Chilean subduction zone (38°Ű18°S). *Pure and Applied Geophysics*, *173*(5), 1431–1449. https://doi.org/10.1007/s00024-016-1280-5

Ogata, Y. (1988). Statistical models for earthquake occurrences and residual analysis for point processes. *Journal of the American Statistical association*, *83*(401), 9–27. https://doi.org/10.1080/01621459.1988.10478560

Ogata, Y., & Katsura, K. (1993). Analysis of temporal and spatial heterogeneity of magnitude frequency distribution inferred from earthquake catalogues. *Geophysical Journal International*, *113*(3), 727–738. https://doi.org/10.1111/j.1365-246x.1993.tb04663.x

Peltzer, G., Rosen, P., Rogez, F., & Hudnut, K. (1998). Poroelastic rebound along the Landers 1992 earthquake surface rupture. *Journal of Geophysical Research*, *103*(B12), 30,131–30,145. https://doi.org/10.1029/98JB02302

Perfettini, H., Avouac, J.-P., & Ruegg, J.-C. (2005). Geodetic displacements and aftershocks following the 2001 $M_w = 8.4$ Peru earthquake: Implications for the mechanics of the earthquake cycle along subduction zones, *Journal of Geophysical Research*, *110*, B09404. https://doi.org/10.1029/2004JB003522

Peyrat, S., & Favreau, P. (2010). Kinematic and spontaneous rupture models of the 2005 Tarapacá intermediate depth earthquake. *Geophysical Journal International*, *181*, 369–381. https://doi.org/10.1111/j.1365-246x.2009.04493.x

Peyrat, S., Campos, J., De Chabalier, J.-B., Perez, A., Bonvalot, S., Bouin, M.-P., ... Vilotte, J. P. (2006). Tarapacá intermediate-depth earthquake (M_w 7.7, 2005, Northern Chile): A slab-pull event with horizontal fault plane constrained from seismologic and geodetic observations. *Geophysical Research Letters*, *33*, L2230. https://doi.org/10.1029/2006GL027710

Peyrat, S., Madariaga, R., Buforn, E., Campos, J., Asch, G., & Vilotte, J. (2010). Kinematic rupture process of the 2007 Tocopilla earthquake and its main aftershocks from teleseismic and strong-motion data. *Geophysical Journal International*, *182*, 1411–1430. https://doi.org/10.1111/j.1365-246x.2010.04685.x

Pritchard, M., & Simons, M. (2006). An aseismic slip pulse in Northern Chile and along-strike variations in seismogenic behavior. *Journal of Geophysical Research*, *111*, B08405. https://doi.org/10.1029/2006JB004258

Reverso, T., Marsan, D., & Helmstetter, A. (2015). Detection and characterization of transient forcing episodes affecting earthquake activity in the Aleutian Arc system. *Earth and Planetary Science Letters*, *412*, 25–34. https://doi.org/10.1016/j.epsl.2014.12.012

Reverso, T., Marsan, D., Helmstetter, A., & Enescu, B. (2016). Background seismicity in Boso Peninsula, Japan: Long-term acceleration, and relationship with slow slip events. *Geophysical Research Letters*, *43*, 5671–5679. https://doi.org/10.1002/2016GL068524

Ruiz, S., & Madariaga, R. (2011). Determination of the friction law parameters of the M_w 6.7 Michilla earthquake in Northern Chile by dynamic inversion. *Geophysical Research Letters*, *38*, L09317. https://doi.org/10.1029/2011GL047147

Ruiz, S., Metois, M., Fuenzalida, A., Ruiz, J., Leyton, F., Grandin, R., ... Campos, J. (2014). Intense foreshocks and a slow slip event preceded the 2014 Iquique M_w 8.1 earthquake. *Science*, *345*(6201), 1165–1169. https://doi.org/10.1126/science.1256074

Schurr, B., Asch, G., Hainzl, S., Bedford, J., Hoechner, A., Palo, M., ... Vilotte, J.-P. (2014). Gradual unlocking of plate boundary controlled initiation of the 2014 Iquique earthquake. *Nature*, *512*(7514), 299–302. https://doi.org/10.1038/nature13681

Socquet, A., Piña Valdes, J., Jara, J., Cotton, F., Walpersdorf, A., Cotte, N., ... Norabuena, E. (2017). An 8-month slow slip event triggers progressive nucleation of the 2014 Chile megathrust. *Geophysical Research Letters*, *44*, 4046–4053. https://doi.org/10.1002/2017GL073023

Spence, W. (1987). Slab pull and the seismotectonics of subducting lithosphere. *Reviews of Geophysics*, *25*(1), 55–69. https://doi.org/10.1029/RG025i001p00055

Utsu, T., & Seki, A. (1955). A relation between the area of aftershock region and the energy of main shock. *Journal of Seismological Society of Japan*, *7*, 233–240. https://doi.org/10.4294/zisin1948.7.4233

Yagi, Y., Okuwaki, R., Enescu, B., Hirano, S., Yamagami, Y., Endo, S., & Komoro, T. (2014). Rupture process of the 2014 Iquique Chile earthquake in relation with the foreshock activity. *Geophysical Research Letters*, *41*, 4201–4206. https://doi.org/10.1002/2014GL060274

Yokota, Y., & Koketsu, K. (2015). A very long-term transient event preceding the 2011 Tohoku earthquake. *Nature communications*, *6*, 5934. https://doi.org/10.1038/ncomms6934